Biointerface Research in Applied Chemistry
Open-Access Journal (ISSN: 2069-5837)

*Article*
**Volume 16, Issue 2, 2026, 44**
https://doi.org/10.33263/BRIAC162.044

# Structural Property Relationship to Approximate the Inferred Dielectric Constant of Alkyl-Functionalized $T_8$ - POSS

**Ashwini Yalnaik [1], Sandhya B G [1,*]**

[1] Department of Studies in Mathematics, Davangere University, Davangere, 577007, Karnataka, India
* Correspondence: sandhyascholar2023@gmail.com;

**Received: 23.11.2025; Accepted: 19.01.2026; Published: 15.04.2026**

**Abstract:** This study introduces a new topological index, the Neighbor Eccentric Distance Sum index, designed to capture both local and overall structural features of molecular graphs. The aim is to understand how this index relates to established measures and how well it reflects structural behavior. We derive its basic bounds, obtain exact expressions for several familiar classes of planar and bipartite graphs, and establish its mathematical connection with the Eccentric-Distance Sum index. To demonstrate its practical use, the index is applied to alkyl-functionalized $T_8$ polyhedral-oligomeric silsesquioxane molecules for estimating their dielectric constants. Moreover, dielectric constants are not fixed universal values; they vary with molecular environment, packing density, morphology, and measurement conditions. Here, we employ a ratio-based approach to examine how the dielectric constant varies in molecular structure. The findings are reflected through topological indices where dielectric behavior is assumed across a homologous series. The calculated values show a consistent relation between the new index and the observed dielectric response of these molecules. The results indicate that the proposed index effectively describes structure-property relationships compared to other commonly used indices, such as the Wiener index and the Eccentric-Distance Sum index. Overall, the findings suggest that this index can serve as a useful tool in quantitative structure-property studies and may help improve the understanding of how graph-theoretical structure influences material behavior.

**Keywords:** POSS; silsesquioxane; dielectric constant; eccentricity; eccentric-distance sum.



## 1. Introduction

Chemical graph theory [1] offers a mathematical way to study molecular structures by using graphs, where atoms are treated as vertices and the bonds between them as edges. This approach allows researchers to define numerical quantities called Topological Indices (TI), which describe how the structure of a molecule relates to its physical and chemical properties. These indices have become powerful tools in quantitative structure-property and structure-activity relationship studies, helping to predict and compare molecular behaviors. Many researchers have studied these indices to learn more about different types of graphs. Refer to these citations for further reading on topological indices [2-8].

Among several distance-based indices, the Eccentric-Distance Sum (EDS) index [9] has been widely used because it combines two important parameters, distance and eccentricity, to represent the overall structure of a molecule. However, this index has a limitation: it assigns

values based solely on the eccentricity of each vertex, without accounting for its neighboring vertices. In many molecular systems, the connections around an atom strongly influence how the structure behaves as a whole. This gap motivated the development of an improved index.

To fill this gap, we introduce a new descriptor called the *Neighbor Eccentric Distance Sum index* (NEDS), denoted by $N\xi^{ds}$. This new index modifies the idea of the EDS by including the eccentricities of the vertices directly connected to each vertex. In this way, the measure becomes more sensitive to how atoms are arranged and how their neighboring connections influence the structure. The index does provide a mathematical link between the structure of a molecule and its measurable properties.

In this study, we formally define the neighbor eccentric distance sum index and derive exact expressions for several classes of planar, highly symmetrical bipartite graphs. We also establish relationships between this new index and classical measures such as the Wiener, Zagreb, and EDS indices. Finally, we apply the proposed index to estimate the dielectric constant of alkyl functionalized $T_8$ polyhedral oligomeric silsesquioxane ($T_8$-POSS) molecules. The results show that this index successfully reflects the structural variations that correspond to the observed changes in dielectric behavior.

Alkyl-functionalized $T_8$ polyhedral oligomeric silsesquioxanes consist of a rigid silsesquioxane cage with alkyl groups of different chain lengths attached to it. The dielectric constant of these molecules is influenced by the nature and length of the alkyl groups, since longer alkyl chains are non-polar and increase free volume, which generally lowers the dielectric response. This variation in dielectric behavior is closely related to changes in the molecular structure. The neighbor eccentric distance sum index captures these structural changes by incorporating both the eccentricity of vertices and the influence of their neighbors in the molecular graph. As the alkyl chain length increases, the corresponding change in graph structure is captured by the index, showing a consistent relationship with the assumed dielectric constant trends of alkyl-functionalized T8-POSS molecules.

Moreover, dielectric constants are generally considered approximated values, not exact. They depend on the material's structure, measurement conditions, and theoretical models used, especially in computational studies. As a result, reported values can differ significantly even for chemically similar materials. In such cases, researchers commonly approximate dielectric constants within a physically reasonable range based on known chemical trends, including molecular polarity, chain length, and structural similarity to related compounds. These approximations allow exploratory and comparative studies to examine how structural variations influence dielectric behavior, without claiming experimental validation or predictive accuracy.

Hence, the dielectric constants adopted in this study are assumed from reported online trends and are used for theoretical and comparative purposes only. The justification for employing approximated dielectric constants has been widely discussed in earlier studies which says, accurate experimental dielectric constant data are often unavailable for many organic and molecular systems, leading researchers to employ predictive or estimation methods such as QSPR to fill data gaps [10], and in studies of ionic liquids and similar materials, the limited availability of experimental dielectric constant measurements necessitates the use of computational QSPR models to estimate these values for large sets of compounds [11], quantitative structure–property relationship models have been widely applied to predict dielectric constants of organic molecules when direct experimental data are missing, indicating that approximate values are a standard tool in theoretical studies [12], in polymer research,

machine learning and QSPR approaches are commonly used to estimate dielectric constants because exhaustive experimental measurement is impractical for diverse polymer sets [13].

Overall, the Neighbor Eccentric-Distance Sum index provides a refined mathematical approach for describing molecular structures. It extends the capability of existing distance-based indices and offers a more reliable way to relate molecular graphs with physical and material properties.

## 2. Materials and Methods

This section provides essential definitions and background concepts used throughout this study.

### *2.1. Basic definitions.*

A graph [14] is a mathematical structure $G = (V, E)$ consisting of a non-empty set of vertices $V$ and a set of edges $E$ that connect pairs of vertices.

For a vertex $v \in V(G)$, the degree $d(v)$ of $v$ in $G$ is the number of edges incident with $v$ [14].

For $u, v \in V(G)$, the distance $d(u, v)$ between two vertices in $G$ is the length of the shortest path connecting them [14].

The eccentricity $e(v)$ of a vertex in a graph $G$ is the greatest distance between that vertex and any other vertex in the graph [14].

The status of a vertex $v$ in a connected graph $G$ is defined as $\sigma(v) = \sum_{u \in V(G)} d(u, v)$.

The radius of a connected graph $G$, denoted by $r(G)$, is defined as the minimum of the eccentricities of its vertices.

The diameter of a connected graph $G$ is the maximum among all geodesics in G. And it is denoted by $D=diam(G)$.

### *2.2. Topological indices.*

The Wiener index [8] is the summation of the shortest path distances between all pairs of vertices in a connected graph. Mathematically, it can be written as:

$$W(G) = \sum_{\{u,v\} \subseteq V(G)} d(u, v) \qquad (1)$$

It is used in fields like chemical graph theory, network analysis, and optimization problems. For further in-depth information, refer to [15, 16].

The First Zagreb index [17] of a graph is the sum of the squares of the degrees of all its vertices. Mathematically, it can be written as:

$$M_1(G) = \sum_{v \in V(G)} (d(v))^2 = \sum_{uv \in E(G)} (d(u) + d(v)) \qquad (2)$$

The First Zagreb coindex [18] of a graph is the sum of the degree sums of all pairs of non-adjacent vertices. Mathematically, it can be written as:

$$\overline{M_1}(G) = \sum_{uv \notin E(G)} (d(u) + d(v)) \qquad (3)$$

The Eccentric-Distance Sum index [9] is defined as:

$$\xi^{ds}(G) = \sum_{\{u,v\}\subseteq V(G)}[e(u) + e(v)]d(u,v) \qquad (4)$$

It can be noted that the physical properties of a chemical compound often strongly influence its biological activity. Gupta *et al*. [9] have effectively demonstrated that the Eccentric-Distance Sum index exhibits strong discriminative capabilities and outstanding predictive accuracy in relation to biological and physical properties. For a detailed exploration of the EDS under various parameter constraints, refer to [19-25].

Nowadays, the neighbor degree concept is increasingly used by researchers to understand the intricate relationships and connectivity patterns within complex networks. In modern graph theory, this concept is applied to analyze how the degree distributions of neighboring vertices influence overall network behavior. Relevant studies of the neighbor degree concept and its topological indices can be found in [26-28].

Inspired by the EDS index and the neighbor degree concept, we present here a new topological index, the Neighbor Eccentric Distance Sum index, which is defined as follows:

$$N\xi^{ds}(G) = \sum_{\{u,v\}\subseteq V(G)}[\omega_e(u) + \omega_e(v)]d(u,v) \qquad (5)$$

where, $\omega_e(u) = \sum_{v\in N(u)} e(v)$ and $\omega_e(v) = \sum_{u\in N(v)} e(u)$are neighbors eccentricity sum of *u* and *v*, respectively, *N(u)* denote the set of neighbors of *u* and *N(v)* denote the set of neighbors of *v* $\forall u, v \in V(G)$.

**Example:** Let $\boldsymbol{G} = \{\{\boldsymbol{v_1}, \boldsymbol{v_2}\}, \{\boldsymbol{v_2}, \boldsymbol{v_3}\}, \{\boldsymbol{v_3}, \boldsymbol{v_4}\}, \{\boldsymbol{v_4}, \boldsymbol{v_2}\}\}$, then:

$$\boldsymbol{N\xi^{ds}(G)} = [\boldsymbol{\omega_e(v_1)} + \boldsymbol{\omega_e(v_2)}]\boldsymbol{d(v_1, v_2)} + [\boldsymbol{\omega_e(v_1)} + \boldsymbol{\omega_e(v_3)}]\boldsymbol{d(v_1, v_3)}$$

$$+[\boldsymbol{\omega_e(v_1)} + \boldsymbol{\omega_e(v_4)}]\boldsymbol{d(v_1, v_4)} + [\boldsymbol{\omega_e(v_2)} + \boldsymbol{\omega_e(v_3)}]\boldsymbol{d(v_2, v_3)}$$

$$+[\boldsymbol{\omega_e(v_2)} + \boldsymbol{\omega_e(v_4)}]\boldsymbol{d(v_2, v_4)} + [\boldsymbol{\omega_e(v_3)} + \boldsymbol{\omega_e(v_4)}]\boldsymbol{d(v_3, v_4)}$$

=[1+6]1+[1+3]2+[1+3]2+[6+3]1+[6+3]1+[3+3]1

=47

*2.3. Chemical background.*

POSS (polyhedral oligomeric silsesquioxane) [29] compounds are hybrid materials with a distinctive cage-like 3D structure. The general nomenclature is formulated as $(RSiO_{1.5})_n$ where *R* represents an organic group, and *n* represents the number of repeating units. These molecules combine the strength and stability of silicon-oxygen frameworks with the flexibility of organic groups, making them valuable in fields such as materials science, electronics, and nanotechnology.

$T_8$-POSS is a specific type of POSS molecule with eight silicon-oxygen bonds, forming a cubic structure with the general formula $(RSiO_{1.5})_8$, where *R* is an organic or functional group attached to the *Si* atom as shown in Figure 1 [29]. While POSS materials, including $T_8$-POSS, typically exhibit a low dielectric constant, they provide an aid to modify the dielectric properties of composite materials. By blending $T_8$-POSS with other materials or incorporating it into different materials, it is possible to optimize the overall dielectric behavior for specific applications, such as in electronic devices and insulating materials.

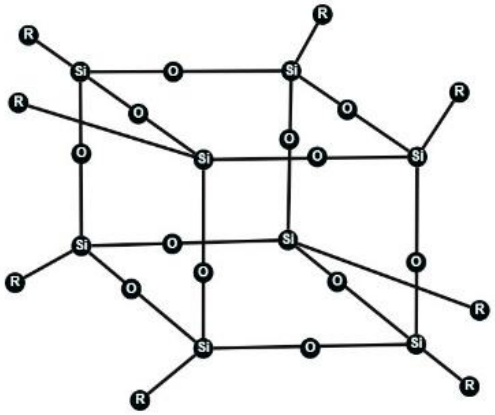

**Figure 1.** Octahedral silsesquioxane $(RSiO_{1.5})_8$ or $T_8$-POSS.

The dielectric constant [30], also known as the relative permittivity, is a measure of a material's ability to store electrical energy in an electric field compared to vacuum. It indicates how much a material can reduce the effective electric field within it by polarizing in response to an applied voltage. A higher dielectric constant means the material can store more charge, making it useful in capacitors and insulating applications. It is a dimensionless quantity, typically denoted by $\varepsilon_r$, and is defined as the ratio of a material's permittivity $(\varepsilon)$ to the permittivity of free space $\varepsilon_0$. For further study, the reader may refer to the following link [31].

The alkyl-functionalized $T_8$-POSS contains $R$ as a non-polar alkyl group $C_nH_{2n+1}$ where n=1, 2, 3, …, 20 as shown in Figure 2. The dielectric constant generally decreases as the alkyl chain length increases. This occurs because alkyl groups are non-polar, reducing overall polarizability and dipole interactions compared to more polar substituents like hydroxyl (-*OH*) or amino (-$NH_2$). Additionally, longer alkyl chains create more free volume and steric hindrance, which lowers material density and decreases the dielectric constant. The hydrophobic nature of alkyl-functionalized POSS further reduces interactions with polar molecules, contributing to this decline. As a result, short-chain alkyl groups (e.g., methyl, ethyl) have relatively higher dielectric constants, whereas long-chain alkyl groups (e.g., octyl, dodecyl) lead to lower dielectric constants due to increased free volume and reduced polarizability.

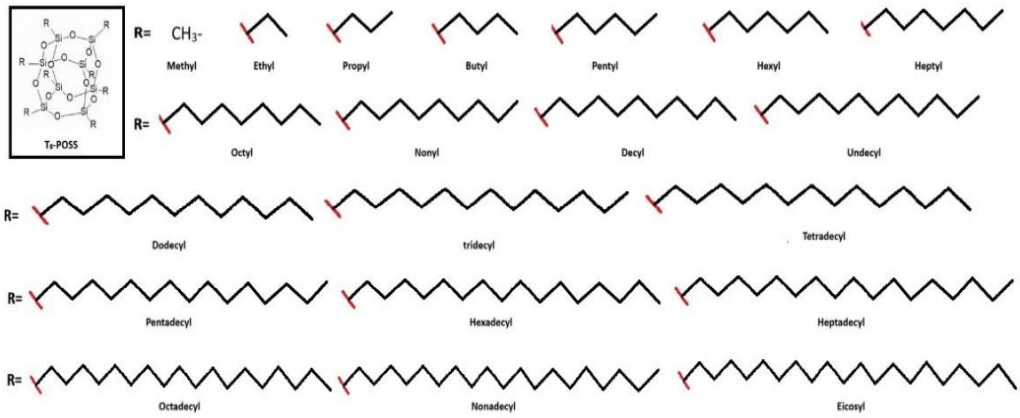


**Figure 2.** $T_8$-POSS with *R*=alkyl group.

For instance, a study on POSS-polyimide nanocomposites reported dielectric constants as low as 2.3, achieved by incorporating POSS-diamine into the polyimide network [32]. Another study on waterborne polyurethane/POSS composites observed a decrease in the dielectric constant from about 2.9 to 2.0 with increasing POSS content [33].

These findings suggest that POSS derivatives can effectively lower the dielectric constant of polymer composites, but specific dielectric constant values for pure alkyl-functionalized $T_8$-POSS molecules are predicted estimates, not experimentally measured values, and not comprehensively reported in any literature. According to available data [34], the dielectric constants of materials derived from non-polar group-functionalized octahedral silsesquioxanes generally lie between 1.0 and 3.0

In section 3, we compute the $N\xi^{ds}$ for a specific class of planar graphs. Section 4 is devoted to the computation of both $\xi^{ds}$ and $N\xi^{ds}$ for certain classes of highly symmetrical bipartite graphs. In section 5, we establish lower and upper bounds for the $N\xi^{ds}$. And later, we explore the relationship between the $\xi^{ds}$ and $N\xi^{ds}$ for selected graph families. Finally, Section 6 comprehensively discusses the correlation and regression findings of the dielectric constant of alkyl-functionalized $T_8$-POSS molecules.

## 3. Results and Discussion

### *3.1. Computation of NEDS index for some classes of planar graphs.*

*Definition 3.1.1* A cycle graph is a graph in which the vertices are connected in a circular form, with the first and last vertices also joined. Each vertex is connected to exactly two other vertices.

**Theorem 3.1.1** For any cycle graph $C_n$, $n \geq 4$,

$$N\xi^{ds}(C_n) = \begin{cases} \frac{n^4}{4} & : if\ n\ is\ even \\ \frac{n(n-1)^2(n+1)}{4} & : if\ n\ is\ odd \end{cases}$$

***Proof:*** Let $C_n$ be a cycle graph. For any cycle graph $C_n$, there are $\binom{n}{2}$ pairs of vertices. For any $v_i \in V(G)$, the eccentricity $e(v_i) = \frac{n}{2}$ is even if $n$ is even and $e(v_i) = \frac{n-1}{2}$ if $n$ is odd with exactly 2 neighbors each.

If $n$ is even:

$$\begin{aligned} N\xi^{ds}(C_n) &= \sum_{\{u,v\}\subseteq V(C_n)} [\omega_e(u) + \omega_e(v)]d(u,v) \\ &= \sum_{\{u,v\}\subseteq V(C_n)} \left[2\left(\frac{n}{2}\right) + 2\left(\frac{n}{2}\right)\right] d(u,v) \\ &= \sum_{\{u,v\}\subseteq V(C_n)} (2n)d(u,v) \\ N\xi^{ds}(C_n) &= 2n(W(C_n)) \end{aligned}$$

If $n$ is odd:

$$\begin{aligned} N\xi^{ds}(C_n) &= \sum_{\{u,v\}\subseteq V(C_n)} [\omega_e(u) + \omega_e(v)]d(u,v) \\ &= \sum_{\{u,v\}\subseteq V(C_n)} \left[2\left(\frac{n-1}{2}\right) + 2\left(\frac{n-1}{2}\right)\right] d(u,v) \\ &= \sum_{\{u,v\}\subseteq V(C_n)} [2(n-1)]d(u,v) \\ N\xi^{ds}(C_n) &= 2(n-1)(W(C_n)) \end{aligned}$$

**Corollary 3.1.1** For any cycle graph $C_n$, $n \geq 4$, $N\xi^{ds}(C_n) = 2\xi^{ds}(C_n)$.

**Definition 3.1.2** A wheel graph, denoted by $W_{1+n}$, is obtained by taking a cycle graph $C_n$ and adding one new vertex, called the central vertex, which is connected to all vertices of the cycle.

**Theorem 3.1.2** For any wheel graph $W_{1+n}$, $n \geq 4$,

$$N\xi^{ds}(W_{1+n}) = 3n[4n-5]$$

***Proof:*** Let us partition the set of $\frac{n(n+1)}{2}$ vertex pairs of wheel graph $W_{1+n}$ into three distinct sets $P_1$, $P_2$, and $P_3$ as shown in Table 1.

**Table 1.** Eccentricities, neighbor eccentricity sums, distances, and cardinality-based vertex pairs of the wheel graph.

| Vertex pair | $e(v_i)$ | $e(v_j)$ | $\omega_e(v_i)$ | $\omega_e(v_j)$ | $d(v_i, v_j)$ | Vertex pair cardinality |
|---|---|---|---|---|---|---|
| $\{v_i, v_j\} \in P_1$ | 1 | 2 | $2n$ | 5 | 1 | $\|P_1\| = n$ |
| $\{v_i, v_j\} \in P_2$ | 2 | 2 | 5 | 5 | 1 | $\|P_2\| = n$ |
| $\{v_i, v_j\} \in P_3$ | 2 | 2 | 5 | 5 | 2 | $\|P_3\| = n\left(\frac{n-3}{2}\right)$ |

By substituting the values from Table 1 in Equation (5), we obtain:

$$N\xi^{ds}(W_{1+n}) = 3n[4n-5]$$

**Corollary 3.1.2** For any wheel graph $W_{1+n}$, $n \geq 4$, $N\xi^{ds}(W_{1+n}) = 3\xi^{ds}(W_{1+n})$.

***Definition 3.1.3*** A friendship graph, denoted by $F_n$, is a simple connected graph constructed from $n$ triangles by merging one vertex of each triangle into a single common vertex. As a result, the graph has one vertex of degree $2n$, while all remaining vertices have degree 2.

**Theorem 3.1.3** For any friendship graph $F_n$, $n \geq 2$,

$$N\xi^{ds}(F_n) = 4n[8n-3]$$

***Proof:*** Let us partition the set of $n(2n+1)$ vertex pairs of friendship graph $F_n$ into three distinct sets $P_1, P_2$ & $P_3$ as shown in Table 2.

**Table 2.** Eccentricities, neighbor eccentricity sums, distances, and cardinality-based vertex pairs of the friendship graph.

| Vertex pair | $e(v_i)$ | $e(v_j)$ | $\omega_e(v_i)$ | $\omega_e(v_j)$ | $d(v_i, v_j)$ | Vertex pair cardinality |
|---|---|---|---|---|---|---|
| $\{v_i, v_j\} \in P_1$ | 1 | 2 | $4n$ | 3 | 1 | $\|P_1\| = 2n$ |
| $\{v_i, v_j\} \in P_2$ | 2 | 2 | 3 | 3 | 1 | $\|P_2\| = n$ |
| $\{v_i, v_j\} \in P_3$ | 2 | 2 | 3 | 3 | 2 | $\|P_3\| = 2n(n-1)$ |

By substituting the values from Table 2 in Equation (5), we obtain:

$$N\xi^{ds}(F_n) = 4n[8n-3]$$

**Corollary 3.1.3** For any friendship graph $F_n$, $n \geq 2$, $N\xi^{ds}(F_n) = 2\xi^{ds}(F_n)$.

*3.2. Computation of EDS and NEDS indices for some highly symmetrical bipartite graphs.*

***Definition 3.2.1*** A crown graph, denoted by $H_{n,n}$, is a bipartite graph formed from $K_{n,n}$ by removing a perfect matching. It has two sets of $n$ vertices, and each vertex is connected to all vertices in the other set except one.

**Theorem 3.2.1** For any crown graph $H_{n,n}$, $n \geq 3$

$$\xi^{ds}(H_{n,n}) = 18n^2$$
$$N\xi^{ds}(H_{n,n}) = (n-1)18n^2$$

***Proof:*** Let us partition the set of $n(2n-1)$ vertex pairs of crown graph $H_{n,n}$ into three distinct sets $P_1$, $P_2$, and $P_3$ as shown in Table 3.

**Table 3.** Eccentricities, neighbor eccentricity sums, distances, and cardinality-based vertex pairs of the crown graph.

| Vertex pair | $e(v_i)$ | $e(v_j)$ | $\omega_e(v_i)$ | $\omega_e(v_j)$ | $d(v_i, v_j)$ | Vertex pair cardinality |
|---|---|---|---|---|---|---|
| $\{v_i, v_j\} \in P_1$ | 3 | 3 | 3(n-1) | 3(n-1) | 1 | $\lvert P_1 \rvert = n(n-1)$ |
| $\{v_i, v_j\} \in P_2$ | 3 | 3 | 3(n-1) | 3(n-1) | 2 | $\lvert P_2 \rvert = n(n-1)$ |
| $\{v_i, v_j\} \in P_3$ | 3 | 3 | 3(n-1) | 3(n-1) | 3 | $\lvert P_3 \rvert = n$ |

By substituting the values from Table 3 in Equation (4) and Equation (5), we obtain:

$$\xi^{ds}(H_{n,n}) = 18n^2 \& N\xi^{ds}(H_{n,n}) = (n-1)18n^2$$

**Corollary 3.2.1** For any crown graph $H_{n,n}$, $n \geq 3, N\xi^{ds}(H_{n,n}) = (n-1)\xi^{ds}(H_{n,n})$.

***Definition 3.2.2*** A cocktail party graph, denoted by $CP_{n,n}$, is a simple graph formed from the complete graph $K_{2n}$ by deleting a perfect matching. It has $2n$ vertices, and each vertex is adjacent to all other vertices except exactly one, making it a regular graph of degree $2n-2$.

**Theorem 3.2.2** For any cocktail party graph $CP_{n,n}$, $n \geq 2$,

$$\xi^{ds}(CP_{n,n}) = 8n^2$$
$$N\xi^{ds}(CP_{n,n}) = (n-1)16n^2$$

***Proof:*** Let us partition the set of $n(2n-1)$ vertex pairs of the cocktail party graph $CP_{n,n}$ into two distinct sets, $P_1$ and $P_2$, as shown in Table 4.

**Table 4.** Eccentricities, neighbor eccentricity sums, distances, and cardinality-based vertex pairs of the cocktail party graph.

| Vertex pair | $e(v_i)$ | $e(v_j)$ | $\omega_e(v_i)$ | $\omega_e(v_j)$ | $d(v_i, v_j)$ | Vertex pair cardinality |
|---|---|---|---|---|---|---|
| $\{v_i, v_j\} \in P_1$ | 2 | 2 | 4(n-1) | 4(n-1) | 1 | $\lvert P_1 \rvert = 2n(n-1)$ |
| $\{v_i, v_j\} \in P_2$ | 2 | 2 | 4(n-1) | 4(n-1) | 2 | $\lvert P_2 \rvert = n$ |

By substituting the values from Table 4 in Equation (4) and Equation (5), we obtain:

$$\xi^{ds}(CP_{n,n}) = 8n^2 \& N\xi^{ds}(CP_{n,n}) = (n-1)16n^2$$

**Corollary 3.2.2** For any cocktail party graph $CP_{n,n}$, $n \geq 2, N\xi^{ds}(CP_{n,n}) = 2(n-1)\xi^{ds}(CP_{n,n})$

**Definition 3.2.3** An $n$-dimensional hypercube graph**,** denoted by $Q_n$, is a simple graph whose vertex set consists of all binary strings of length $n$. Two vertices are joined by an edge if and only if they differ in exactly one coordinate. Consequently, $Q_n$ has $2^n$ vertices, each of degree $n$, and represents the graph structure of an $n$-dimensional cube.

**Theorem 3.2.3** For any hypercube graph $Q_n$,

$$\xi^{ds}(Q_n) = 2n \sum_{d=1}^{n} \left[ d \binom{n}{d} 2^{n-d} \right]$$

$$N\xi^{ds}(Q_n) = 2n^2 \sum_{d=1}^{n} \left[ d \binom{n}{d} 2^{n-d} \right]$$

***Proof:*** Let $Q_n$ be a hypercube graph consisting of $\binom{2^n}{2}$ pairs of vertices, and any vertex $v \in V(Q_n)$ has $n$ neighbors, each with eccentricity $n$. The number of vertex pairs at the distance $d$ is given in Table 5, where $1 \leq d \leq n$.

**Table 5.** Cardinality of vertex pairs at distance d.

| Distance | Number of vertex pairs at distance *d* |
|---|---|
| d=1 | $n2^{n-1}$ |
| d=2 | $\binom{n}{2}2^{n-2}$ |
| d=3 | $\binom{n}{3}2^{n-3}$ |
| d=4 | $\binom{n}{4}2^{n-4}$ |
| d=5 | $\binom{n}{5}2^{n-5}$ |
| d=n-1 | $\binom{n}{n-1}2$ |
| d=n | 1 |

Therefore:

$$\xi^{ds}(Q_n) = \binom{n}{1}2^{n-1}(2n)(1) + \binom{n}{2}2^{n-2}(2n)(2) + \binom{n}{3}2^{n-3}(2n)(3) + \binom{n}{4}2^{n-4}(2n)(4)$$

$$+\ldots+\binom{n}{n-1}2^{n-(n-1)}(2n)(n-1) + \binom{n}{n}2^{n-n}(2n)(n)\xi^{ds}(Q_n) \;= 2n\sum_{d=1}^{n}\left[d\binom{n}{d}2^{n-d}\right]$$

And:

$$N\xi^{ds}(Q_n) = \binom{n}{1}2^{n-1}[(n)(n)+(n)(n)](1) + \binom{n}{2}2^{n-2}[(n)(n)+(n)(n)](2)$$

$$+\binom{n}{3}2^{n-3}[(n)(n)+(n)(n)](3) + \binom{n}{4}2^{n-4}[(n)(n)+(n)(n)](4)$$

$$+\ldots+\binom{n}{n-1}2^{n-(n-1)}[(n)(n)+(n)(n)](n-1) + \binom{n}{n}2^{n-n}[(n)(n)+(n)(n)](n)$$

$$N\xi^{ds}(Q_n) = 2n^2 \sum_{d=1}^{n} \left[ d \binom{n}{d} 2^{n-d} \right]$$

**Corollary 3.2.3** For any hypercube graph $Q_n$, $N\xi^{ds}(Q_n) = n\xi^{ds}(Q_n)$.

***Definition 3.2.4*** A star graph**,** denoted by $S_{1,n}$, is a simple graph consisting of one central vertex connected to n distinct outer vertices. The outer vertices are not adjacent to each other, and the central vertex has degree *n*, while each outer vertex has degree *1*.

**Theorem 3.2.4** For any star graph $S_{1,n}$, $n \geq 2$,

$$\xi^{ds}(S_{1,n}) = n(4n-1)$$

$$N\xi^{ds}(S_{1,n}) = n(4n-1)$$

***Proof:*** Let us partition the set of $\frac{n(n+1)}{2}$ vertex pairs of star graph $S_{1,n}$ into two distinct sets $P_1$ & $P_2$ as shown in Table 6.

**Table 6.** Eccentricities, neighbor eccentricity sums, distances, and cardinality-based vertex pairs of the star graph.

| Vertex pair | $e(v_i)$ | $e(v_j)$ | $\omega_e(v_i)$ | $\omega_e(v_j)$ | $d(v_i, v_j)$ | Vertex pair cardinality |
|---|---|---|---|---|---|---|
| $\{v_i, v_j\} \in P_1$ | 1 | 2 | $2n$ | 1 | 1 | $\lvert P_1 \rvert = n \; \lvert P_1 \rvert = n$ |
| $\{v_i, v_j\} \in P_2$ | 2 | 2 | 1 | 1 | 2 | $\lvert P_2 \rvert = \frac{n(n-1)}{2}$ |

By substituting the values from Table 6 in Equation (4) and Equation (5), we obtain:

$$\xi^{ds}(S_{1,n}) = n(4n-1) \& N\xi^{ds}(S_{1,n}) = n(4n-1)$$

**Corollary 3.2.4** For any star graph $S_{1,n}$, $n \geq 2, N\xi^{ds}(S_{1,n}) = \xi^{ds}(S_{1,n})$.

***Definition 3.2.5*** A complete bipartite graph**,** denoted by $K_{m,n}$, is a graph whose vertex set can be divided into two disjoint parts of sizes *m* and *n*, such that every vertex in one part is connected to all vertices in the other part, and there are no edges between vertices within the same part.

**Theorem 3.2.5** For any complete bipartite graph $K_{m,n}$, $m, n \geq 2$,

$$\xi^{ds}(K_{m,n}) = 4m^2 + 4n^2 + 4mn - 4m - 4n$$
$$N\xi^{ds}(K_{m,n}) = 2mn[3n + 3m - 4]$$

***Proof:*** Let us partition the set of $\frac{(m+n)(m+n-1)}{2}$ vertex pairs of a complete bipartite graph $K_{m,n}$ into three distinct sets P1, P2, and P3 as shown in Table 7.

**Table 7.** Eccentricities, neighbor eccentricity sums, distances, and cardinality-based vertex pairs of a complete bipartite graph.

| Vertex pair | $e(v_i)$ | $e(v_j)$ | $\omega_e(v_i)$ | $\omega_e(v_j)$ | $d(v_i, v_j)$ | Vertex pair cardinality |
|---|---|---|---|---|---|---|
| $\{v_i, v_j\} \in P_1$ | 2 | 2 | $2n$ | $2m$ | 1 | $\lvert P_1 \rvert = mn$ |
| $\{v_i, v_j\} \in P_2$ | 2 | 2 | $2n$ | $2n$ | 2 | $\lvert P_2 \rvert = \frac{m(m-1)}{2}$ |
| $\{v_i, v_j\} \in P_3$ | 2 | 2 | $2m$ | $2m$ | 2 | $\lvert P_3 \rvert = \frac{n(n-1)}{2}$ |

By substituting the values from Table 7 in Equation (4) and Equation (5), we obtain:

$$\boldsymbol{\xi^{ds}(K_{m,n}) = 4m^2 + 4n^2 + 4mn - 4m - 4n \ \& \ N\xi^{ds}(K_{m,n}) = 2mn[3n + 3m - 4]}$$

*3.3. Upper and lower bounds for NEDS index.*

**Definition 3.3.1** A complete graph**,** denoted by $K_n$, is a simple graph with *n* vertices in which every pair of distinct vertices is connected by an edge.

**Lemma 3.3.1** The neighbor eccentric-distance sum index of the complete graph $K_n$ (D=1) is:

$$N\xi^{ds}(K_n) = M_1(K_n)$$

***Proof:*** Let $K_n$ be a complete graph, which has $\binom{n}{2}$ pairs of vertices and any vertex $v \in V(K_n)$ has *n-1* neighbors, each with eccentricity *1* $d(v_i, v_j) = 1 \forall v_i, v_j \in V(K_n)$.

Thus:

$$N\xi^{ds}(K_n) = \sum_{\{u,v\}\subseteq V(K_n)} [\omega_e(u) + \omega_e(v)]d(u,v)$$
$$= \sum_{\{u,v\}\subseteq V(K_n)} [(n-1)(1) + (n-1)(1)]d(u,v)$$
$$= 2(n-1) \sum_{\{u,v\}\subseteq V(K_n)} d(u,v) = 2(n-1)(W(K_n))$$
$$= 2(n-1)\left[\frac{1}{2}\sum_{u\in V(K_n)} \sigma(u)\right]$$

Since the status of all vertices in a complete graph is *n-1*. Therefore:

$$N\xi^{ds}(K_n) = M_1(K_n)$$

**Corollary 3.3.1** For any complete graph $K_n$ $N\xi^{ds}(K_n) = (n-1)\xi^{ds}(K_n)$.

**Theorem 3.3.1** For every connected graph G with order n, size m, $r(G) \geq 2$,
$2M_1(G) + 4\overline{M_1}(G) \leq N\xi^{ds}(G) \leq diam(G)\left[M_1(G) + diam(G)\overline{M_1}(G)\right]$

The equality on both sides holds if and only if r(G)= diam(G)=2, where *G* is a 2-equieccentric graph.

***Proof:*** For any connected graph *G* with $\binom{n}{2}$ vertex pairs, $d(u,v) = 1$ if *u* and *v* are adjacent to each other.

Let us first prove the lower bound. For any graph *G* $r(G) \geq 2$, the minimum value of *d(u,v)* is *2* if *u* and *v* are not adjacent to each other. And the minimum value of eccentricity of each vertex *u* is at least 2. Therefore:

$$N\xi^{ds}(G) = \sum_{\{u,v\}\subseteq V(G)} [\omega_e(u) + \omega_e(v)]d(u,v)$$
$$\geq \sum_{uv\in E(G)} \left[\big(d(u)\big)(2) + \big(d(v)\big)(2)\right](1)$$
$$+ \sum_{uv\notin E(G)} \left[\big(d(u)\big)(2) + \big(d(v)\big)(2)\right](2)$$
$$= 2\sum_{uv\in E(G)} [d(u) + d(v)] + 4\sum_{uv\notin E(G)} [d(u) + d(v)]$$

$$N\xi^{ds}(G) = 2M_1(G) + 4\overline{M_1}(G)$$

Now we prove the upper bound. For any graph *G* with $diam(G) \geq 2$, the distance between non-adjacent pairs of vertices is at most equal to the diameter $diam(G)$, and their respective eccentricities are also considered to be $diam(G)$. Therefore:

$$N\xi^{ds}(G) = \sum_{\{u,v\}\subseteq V(G)} [\omega_e(u) + \omega_e(v)]d(u,v)$$
$$\leq \sum_{uv\in E(G)} \big[\big(d(u)\big)\big(diam(G)\big) + \big(d(v)\big)\big(diam(G)\big)\big](1)$$
$$+ \sum_{uv\notin E(G)} \big[\big(d(u)\big)\big(diam(G)\big) + \big(d(v)\big)\big(diam(G)\big)\big]\big(diam(G)\big)$$
$$= diam(G) \sum_{uv\in E(G)} [d(u) + d(v)] + \big(diam(G)\big)^2 \sum_{uv\notin E(G)} [d(u) + d(v)]$$
$$= diam(G)M_1(G) + \big(diam(G)\big)^2\overline{M_1}(G)$$
$$N\xi^{ds}(G) = diam(G)\big[M_1(G) + diam(G)\overline{M_1}(G)\big]$$

*3.4. Graphical representation of alkyl-functionalized $T_8$-POSS and chemical applicability of the indices.*

For our study, we consider the molecular structure of alkyl-functionalized octahedral silsesquioxanes $(C_nH_{2n+1}SiO_{1.5})_8$ where carbon, silicon, and oxygen are represented as atoms (nodes) followed by bonds represented as edges, whereas hydrogen atom bonds are neglected. The study focuses on deriving a formula for calculating the dielectric constant of these chemical compound groups.

The quantitative structure-property relationship (QSPR) analysis of alkyl-functionalized $T_8$-POSS molecules has been extended to investigate their dielectric constants from methyl to eicosyl derivatives. Dielectric constant values are approximated because of the material's imperfections, anisotropy, temperature-dependent behavior, and they show variation with frequency and applied field strength. Since experimental or reported dielectric constant values for these molecules are not available in the literature, the present study assumes values within the range of 1.0-3.0 based on general trends observed in related online sources. For each molecule, one representative value $(\varepsilon_r^a)$ is selected within the assumed range (see Table 8).

**Table 8.** Assumed range $(\varepsilon_r^{range})$ and assumed single value $(\varepsilon_r^a\ \varepsilon_r^a)$ of the dielectric constant between the range of alkyl-functionalized octahedral silsesquioxanes $(C_nH_{2n+1}SiO_{1.5})_8$ for n=1,2,3,…,20.

| No. of C atoms 'n' | Alkyl group$(C_nH_{2n+1})$ | $(C_nH_{2n+1}SiO_{1.5})_8$ | $\varepsilon_r^{range}$ | $\varepsilon_r^a$ |
|---|---|---|---|---|
| 1 | Methyl $(CH_3-)$ | $\boldsymbol{(CH_3SiO_{1.5})_8}$ | 2.5 – 3.0 | 2.6 |
| 2 | Ethyl $(C_2H_5-)$ | $(C_2H_5SiO_{1.5})_8$ | 2.4 – 3.0 | 2.5 |
| 3 | Propyl $(C_3H_7-)$ | $(C_3H_7SiO_{1.5})_8$ | 2.3 – 2.8 | 2.4 |
| 4 | Butyl $(C_4H_9-)$ | $(C_4H_9SiO_{1.5})_8$ | 2.2 – 2.7 | 2.3 |
| 5 | Pentyl $(C_5H_{11}-)$ | $(C_5H_{11}SiO_{1.5})_8$ | 2.1 – 2.6 | 2.2 |
| 6 | Hexyl $(C_6H_{13}-)$ | $(C_6H_{13}SiO_{1.5})_8$ | 2.1 – 2.5 | 2.2 |
| 7 | Heptyl $(C_7H_{15}-)$ | $(C_7H_{15}SiO_{1.5})_8$ | 2.0 – 2.4 | 2.1 |
| 8 | Octyl $(C_8H_{17}-)$ | $(C_8H_{17}SiO_{1.5})_8$ | 2.0 – 2.3 | 2.1 |
| 9 | Nonyl $(C_9H_{19}-)$ | $(C_9H_{19}SiO_{1.5})_8$ | 1.9 – 2.2 | 2.0 |
| 10 | Decyl $(C_{10}H_{21}-)$ | $(C_{10}H_{21}SiO_{1.5})_8$ | 1.9 – 2.1 | 2.0 |
| 11 | Undecyl $(C_{11}H_{23}-)$ | $(C_{11}H_{23}SiO_{1.5})_8$ | 1.8 – 2.0 | 1.9 |
| 12 | Dodecyl $(C_{12}H_{25}-)$ | $(C_{12}H_{25}SiO_{1.5})_8$ | 1.8 – 2.0 | 1.9 |
| 13 | Tridecyl $(C_{13}H_{27}-)$ | $(C_{13}H_{27}SiO_{1.5})_8$ | 1.7 – 1.9 | 1.8 |
| 14 | Tetradecyl $(C_{14}H_{29}-)$ | $(C_{14}H_{29}SiO_{1.5})_8$ | 1.7 – 1.9 | 1.8 |
| 15 | Pentadecyl $(C_{15}H_{31}-)$ | $(C_{15}H_{31}SiO_{1.5})_8$ | 1.6 – 1.8 | 1.7 |
| 16 | Hexadecyl $(C_{16}H_{33}-)$ | $(C_{16}H_{33}SiO_{1.5})_8$ | 1.6 – 1.8 | 1.7 |
| 17 | Heptadecyl $(C_{17}H_{35}-)$ | $(C_{17}H_{35}SiO_{1.5})_8$ | 1.5 – 1.7 | 1.6 |
| 18 | Octadecyl $(C_{18}H_{37}-)$ | $(C_{18}H_{37}SiO_{1.5})_8$ | 1.5 – 1.7 | 1.6 |
| 19 | Nonadecyl $(C_{19}H_{39}-)$ | $(C_{19}H_{39}SiO_{1.5})_8$ | 1.4 – 1.6 | 1.5 |
| 20 | Eicosyl $(C_{20}H_{41}-)$ | $(C_{20}H_{41}SiO_{1.5})_8$ | 1.4 – 1.6 | 1.5 |

To provide a consistent and rational estimation, the dielectric constant for each molecule is determined using a ratio-based approach, where the ratio is defined as the topological index value of a given molecule divided by that of its preceding *homologous molecule*. Mathematically, this can be expressed as:

$$\varepsilon_r^e((C_nH_{2n+1}SiO_{1.5})_8) = \frac{TI((C_nH_{2n+1}SiO_{1.5})_8)}{TI((C_{n-1}H_{2n-1}SiO_{1.5})_8)} \forall n \in N \quad (6)$$

Here $\varepsilon_r^e$ is the estimated dielectric constant value $(C_nH_{2n+1}SiO_{1.5})_8$ is that of alkyl-functionalized $T_8$-POSS, $(C_{n-1}H_{2n-1}SiO_{1.5})_8$ which is the preceding molecule of every alkyl-functionalized $T_8$-POSS.

This ratio-based formulation is specifically applicable to the homologous series of alkyl-functionalized $T_8$-POSS molecules, where structural continuity exists between successive members. It is not intended for individual or non-homologous compounds.

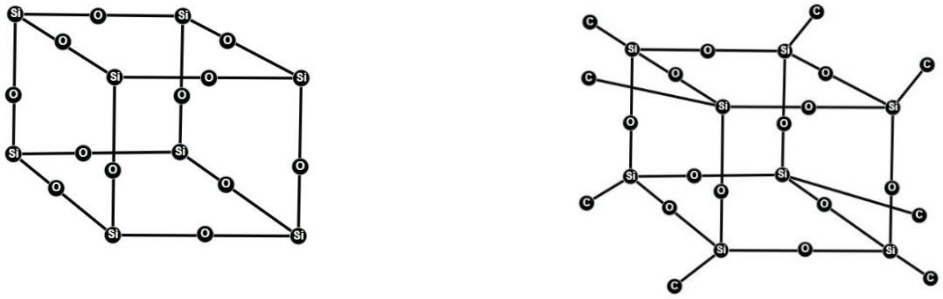

**(a)** **(b)**

**Figure 3. (a)** $(HSiO_{1.5})_8$; **(b)** $(CH_3SiO_{1.5})_8$.

For example, using Python, we obtain the NEDS of Octahydrosilsesquioxane (Figure 3(a) [29]) to be 17568. Similarly, the NEDS of Octamethylsilsesquioxane or methyl $T_8$-POSS (Figure 3(b)) is found to be 41536. The estimated dielectric constant of methyl $T_8$-POSS is calculated as the ratio of its index value to that of its preceding molecule. i.e.:

$$\varepsilon_r^e((CH_3SiO_{1.5})_8) = \frac{NEDS((CH_3SiO_{1.5})_8)}{NEDS((HSiO_{1.5})_8)} = \frac{41536}{17568} = 2.364298725 \quad (7)$$

The same methodology is extended to the remaining indices.

In Table 9, Wiener index, EDS index, and NEDS index are calculated for alkyl-functionalized octahedral silsesquioxanes $(C_nH_{2n+1}SiO_{1.5})_8$ for n=1,2,3,…,20.

**Table 9.** Computed topological indices for alkyl-functionalized octahedral silsesquioxanes $(C_nH_{2n+1}SiO_{1.5})_8$ for n=1,2,3,…,20.

| $(C_nH_{2n+1}SiO_{1.5})_8$ | W | EDS | NEDS |
|---|---|---|---|
| $(CH_3SiO_{1.5})_8$ | 1404 | 19472 | 41536 |
| $(C_2H_5SiO_{1.5})_8$ | 2780 | 47352 | 95280 |
| $(C_3H_7SiO_{1.5})_8$ | 4916 | 99376 | 194960 |
| $(C_4H_9SiO_{1.5})_8$ | 7988 | 186904 | 362624 |
| $(C_5H_{11}SiO_{1.5})_8$ | 12172 | 323520 | 624768 |
| $(C_6H_{13}SiO_{1.5})_8$ | 17644 | 525032 | 1012336 |
| $(C_7H_{15}SiO_{1.5})_8$ | 24580 | 809472 | 1560720 |
| $(C_8H_{17}SiO_{1.5})_8$ | 33156 | 1197096 | 2309760 |
| $(C_9H_{19}SiO_{1.5})_8$ | 43548 | 1710384 | 3303744 |
| $(C_{10}H_{21}SiO_{1.5})_8$ | 55932 | 2374040 | 4591408 |

| $(C_nH_{2n+1}SiO_{1.5})_8$ | W | EDS | NEDS |
|---|---|---|---|
| $(C_{11}H_{23}SiO_{1.5})_8$ | 70484 | 3214992 | 6225936 |
| $(C_{12}H_{25}SiO_{1.5})_8$ | 87380 | 4262392 | 8264960 |
| $(C_{13}H_{27}SiO_{1.5})_8$ | 106796 | 5547616 | 10770560 |
| $(C_{14}H_{29}SiO_{1.5})_8$ | 128908 | 7104264 | 13809264 |
| $(C_{15}H_{31}SiO_{1.5})_8$ | 153892 | 8968160 | 17452048 |
| $(C_{16}H_{33}SiO_{1.5})_8$ | 181924 | 11177352 | 21774336 |
| $(C_{17}H_{35}SiO_{1.5})_8$ | 213180 | 13772112 | 26856000 |
| $(C_{18}H_{37}SiO_{1.5})_8$ | 247836 | 16794936 | 32781360 |
| $(C_{19}H_{39}SiO_{1.5})_8$ | 286068 | 20290544 | 39639184 |
| $(C_{20}H_{41}SiO_{1.5})_8$ | 328052 | 24305880 | 47522688 |

In Table 10, Wiener index ratio, EDS index ratio, and NEDS index ratio are expressed by using the values from Table 9 and the following expressions:

$$W_{ratio} = \varepsilon_r^e((C_nH_{2n+1}SiO_{1.5})_8) = \frac{W((C_nH_{2n+1}SiO_{1.5})_8)}{W((C_{n-1}H_{2n-1}SiO_{1.5})_8)} \quad (8)$$

$$EDS_{ratio} = \varepsilon_r^e((C_nH_{2n+1}SiO_{1.5})_8) = \frac{EDS((C_nH_{2n+1}SiO_{1.5})_8)}{EDS((C_{n-1}H_{2n-1}SiO_{1.5})_8)} \quad (9)$$

$$NEDS_{ratio} = \varepsilon_r^e((C_nH_{2n+1}SiO_{1.5})_8) = \frac{NEDS((C_nH_{2n+1}SiO_{1.5})_8)}{NEDS((C_{n-1}H_{2n-1}SiO_{1.5})_8)} \quad (10)$$

**Table 10.** Assumed dielectric constant ($\varepsilon_r^a$) and calculated the ratio by using topological indices for $(C_nH_{2n+1}SiO_{1.5})_8$ for n=1,2,3,…,20.

| $(C_nH_{2n+1}SiO_{1.5})_8$ | $\varepsilon_r^a$ | $W_{ratio}$ | $EDS_{ratio}$ | $NEDS_{ratio}$ |
|---|---|---|---|---|
| $(CH_3SiO_{1.5})_8$ | 2.6 | 2.2941176471 | 2.651416122 | 2.364298725 |
| $(C_2H_5SiO_{1.5})_8$ | 2.5 | 1.9800569801 | 2.431799507 | 2.2939137134 |
| $(C_3H_7SiO_{1.5})_8$ | 2.4 | 1.7683453237 | 2.0986653151 | 2.0461796809 |
| $(C_4H_9SiO_{1.5})_8$ | 2.3 | 1.6248982913 | 1.8807760425 | 1.8599917932 |
| $(C_5H_{11}SiO_{1.5})_8$ | 2.2 | 1.5237856785 | 1.7309420879 | 1.7229085775 |
| $(C_6H_{13}SiO_{1.5})_8$ | 2.2 | 1.4495563589 | 1.6228733927 | 1.6203390699 |
| $(C_7H_{15}SiO_{1.5})_8$ | 2.1 | 1.3931081387 | 1.5417574548 | 1.5417015694 |
| $(C_8H_{17}SiO_{1.5})_8$ | 2.1 | 1.348901546 | 1.4788602941 | 1.4799323389 |
| $(C_9H_{19}SiO_{1.5})_8$ | 2.0 | 1.3134274339 | 1.4287776419 | 1.4303408146 |
| $(C_{10}H_{21}SiO_{1.5})_8$ | 2.0 | 1.2843758611 | 1.3880157906 | 1.3897590128 |
| $(C_{11}H_{23}SiO_{1.5})_8$ | 1.9 | 1.2601730673 | 1.3542282354 | 1.3559971146 |
| $(C_{12}H_{25}SiO_{1.5})_8$ | 1.9 | 1.2397139776 | 1.3257861917 | 1.3275048121 |
| $(C_{13}H_{27}SiO_{1.5})_8$ | 1.8 | 1.2222018769 | 1.3015264668 | 1.3031593619 |
| $(C_{14}H_{29}SiO_{1.5})_8$ | 1.8 | 1.2070489531 | 1.2805976477 | 1.2821305485 |
| $(C_{15}H_{31}SiO_{1.5})_8$ | 1.7 | 1.1938126416 | 1.2623629978 | 1.2637927698 |
| $(C_{16}H_{33}SiO_{1.5})_8$ | 1.7 | 1.1821537182 | 1.2463372643 | 1.2476665203 |
| $(C_{17}H_{35}SiO_{1.5})_8$ | 1.6 | 1.1718080077 | 1.2321444292 | 1.2333785976 |
| $(C_{18}H_{37}SiO_{1.5})_8$ | 1.6 | 1.1625668449 | 1.2194887756 | 1.2206344951 |
| $(C_{19}H_{39}SiO_{1.5})_8$ | 1.5 | 1.1542633032 | 1.2081346425 | 1.2091988862 |
| $(C_{20}H_{41}SiO_{1.5})_8$ | 1.5 | 1.1467623083 | 1.1978919836 | 1.1988815915 |

The correlation analysis summarized in Table 11 presents the correlation coefficient between the dielectric constant and the selected topological indices. Among them, the NEDS index ratio exhibits the highest correlation (r=0.936734), followed by the EDS index ratio (r=0.915679) and the Wiener index ratio (r=0. 904885).

**Table 11.** Correlation coefficients of the index ratio with the dielectric constant

| Index ratio | Correlation |
|---|---|
| Wiener index ratio | 0.904885 |
| EDS index ratio | 0.915679 |
| NEDS index ratio | 0.936734 |

The corresponding statistical parameters are presented in Table 12. Based on the obtained value of $R^2$, Mean Absolute Error (MAE), and Root Mean Square Error (RMSE), we observe that the regression model using NEDS index ratio shows superior predictive performance ($R^2$=0. 877470, MAE=0. 097271, RMSE=0. 111849).

**Table 12.** Correlation coefficients of the index ratio with the dielectric constant.

| Index ratio | $R^2$ | MAE | RMSE |
|---|---|---|---|
| Wiener index ratio | 0.818816 | 0.117532 | 0.136011 |
| EDS index ratio | 0.838468 | 0.112925 | 0.128423 |
| NEDS index ratio | 0.877470 | 0.097271 | 0.111849 |

The derived linear regression equations for estimating the dielectric constant are expressed as:

Dielectric constant=0.6246 + (0.963748) × Wiener index ratio

Dielectric constant=0.8634 + (0.716668) × EDS index ratio

Dielectric constant=0.6735 + (0.853204) × NEDS index ratio

The linear equations derived from Table 10 were used to generate Figures 4, 5, and 6, which illustrate the corresponding correlation coefficients. The bar chart shown in Figure 7 further presents a comparative analysis of $R^2$ values obtained for the proposed ratio using different indices. Notably, the NEDS index ratio exhibits the highest $R^2$ value among them, indicating its superior performance and significance in QSPR studies.

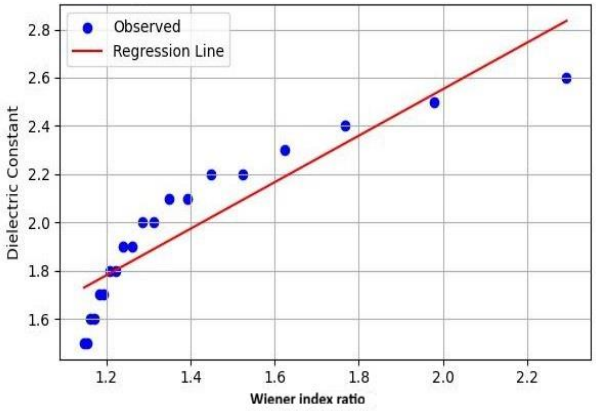


**Figure 4.** Regression of dielectric constant Vs Wiener index ratio.

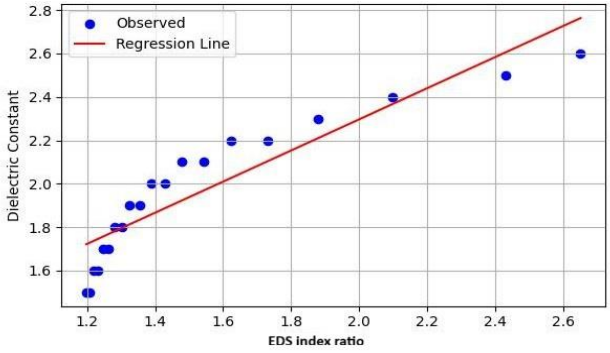


**Figure 5.** Regression of dielectric constant Vs EDS index ratio.

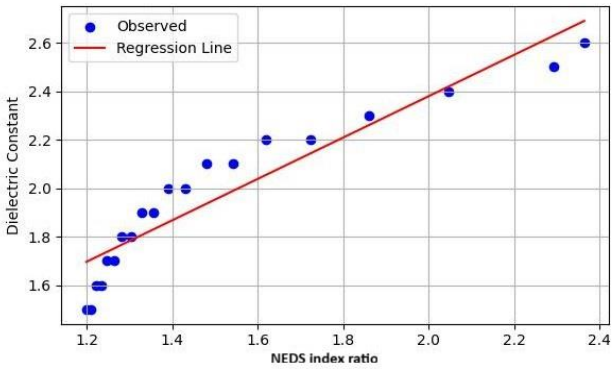


**Figure 6.** Regression of dielectric constant Vs NEDS index ratio.

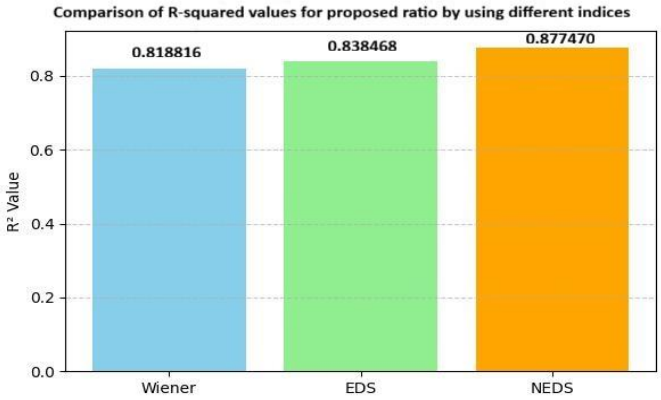


**Figure 7.** $R^2$ comparison bar chart.

## 4. Conclusions

This study introduces the novel NEDS index. We explored its properties and how it relates to the EDS index for different types of graphs. By applying the NEDS index, we showed how it can help to estimate the dielectric constant of alkyl-functionalized $T_8$-POSS, linking molecular structure to molecular properties. This work offers a better understanding of how molecular structure influences physical properties, providing valuable insights for material science. The QSPR analysis of this work reveals a strong linear correlation between the dielectric constant and the studied topological indices. Among the evaluated models, the NEDS index ratio demonstrates the highest correlation and regression accuracy, confirming its reliability in predicting dielectric properties of alkyl-functionalized $T_8$-POSS molecules. A limitation of this work is that the dielectric constants used are assumed values rather than experimentally measured. Therefore, the results are illustrative, and the rationale for adopting assumed dielectric values has been discussed earlier; future work incorporating experimental data is necessary for further validation. Effective medium approximations are used for composites, where exact values are impossible due to inhomogeneity.

## Author Contributions

Conceptualization, S.B.G.; methodology, S.B.G.; validation, S.B.G. and A.Y.; formal analysis, S.B.G.; investigation, A.Y.; data curation, S.B.G.; writing—original draft preparation, S.B.G.; writing—review and editing, S.B.G.; visualization, S.B.G.; supervision, A.Y. All authors have read and agreed to the published version of the manuscript.

## Institutional Review Board Statement

Not applicable.

## Informed Consent Statement

Not applicable.

## Data Availability Statement

Data supporting the findings of this study are available upon reasonable request from the corresponding author.

## Funding

This research received no external funding.

## Acknowledgments

The authors thank the library of Davangere University, Davangere, for the computational resources.

## Conflicts of Interest

The authors declare that they have no conflict of interest.

## References

1. Trinajstić, N. Chemical Graph Theory, 2nd Edition; CRC Press: Boca Raton, USA, **1992**; pp. 1–352, https://doi.org/10.1201/9781315139111.
2. Anbarasan, G.; Narasimhan, D.; Zhang, X. QSPR Analysis of Topological Indices for Nonane and Decane: An Approach to New Open Neighborhood-Edge-Degree. *J. Math.* **2025**, *2025*, 9300802, https://doi.org/10.1155/jom/9300802.
3. Bindusree, A.R.; Nirupadi, K. Computation of SK Group Topological Indices on Certain Graphs. *Palest. J. Math.* **2024**, *13*, 369-377.
4. Granados, A.; Portilla, A.; Quintana, Y.; Tourís, E. New bounds for variable topological indices and applications. *J. Math. Chem.* **2024**, *62*, 1435-1453, https://doi.org/10.1007/s10910-024-01593-w.
5. Hakeem, A.; Katbar, N.M.; Shaikh, H.; Tolasa, F.T.; Abro, O.A. Reverse degree-based topological indices study of molecular structure in triangular ϒ-graphyne and triangular ϒ-graphyne chain. *Front. Phys.* **2024**, *12*, 1422098, https://doi.org/10.3389/fphy.2024.1422098.
6. Priyanka, Y.B. Chemical Graph Theory: Analyzing Molecular Properties Using Topological Indices. *IRE J.* **2024**, *8*, 793–803.
7. Rasheed, M.W.; Mahboob, A.; Hanif, I. Uses of degree-based topological indices in QSPR analysis of alkaloids with poisonous and healthful nature. *Front. Phys.* **2024**, *12*, 1381887, https://doi.org/10.3389/fphy.2024.1381887.
8. Wiener, H. Structural Determination of Paraffin Boiling Points. *J. Am. Chem. Soc.* **1947**, *69*, 17–20, https://doi.org/10.1021/ja01193a005.
9. Gupta, S.; Singh, M.; Madan, A.K. Eccentric distance sum: A novel graph invariant for predicting biological and physical properties. *J. Math. Anal. Appl.* **2002**, *275*, 386-401, https://doi.org/10.1016/S0022-247X(02)00373-6.
10. Liu, J.-P.; Wilding, W.V.; Giles, N.F.; Rowley, R.L. A Quantitative Structure Property Relation Correlation of the Dielectric Constant for Organic Chemicals. *J. Chem. Eng. Data* **2010**, *55*, 41-45, https://doi.org/10.1021/je900518k.
11. Rybinska-Fryca, A.; Sosnowska, A.; Puzyn, T. Prediction of dielectric constant of ionic liquids. *J. Mol. Liq.* **2018**, *260*, 57-64, https://doi.org/10.1016/j.molliq.2018.03.080.

12. Achary, P.G.R. QSPR modelling of dielectric constants of π-conjugated organic compounds by means of the CORAL software. *SAR QSAR Environ. Res.* **2014**, *25*, 507-526, https://doi.org/10.1080/1062936X.2014.899267.
13. Ascencio-Medina, E.; He, S.; Daghighi, A.; Iduoku, K.; Casanola-Martin, G.M.; Arrasate, S.; González-Díaz, H.; Rasulev, B. Prediction of Dielectric Constant in Series of Polymers by Quantitative Structure-Property Relationship (QSPR). *Polymers* **2024**, *16*, 2731, https://doi.org/10.3390/polym16192731.
14. Harary, F. Graph theory. Addison–Wesley Publishing Company: Reading, Massachusetts, USA, **1969**; pp. 1–274.
15. Lin, Z.; Zhou, T. Degree-weighted Wiener index of a graph. *Math. Model. Control* **2024**, *4*, 9–16, https://doi.org/10.3934/mmc.2024002.
16. Subashini, G.; Kannan, K.; Menaga, A. Exponential Wiener index of some silicate networks. *Sci. Rep.* **2024**, *14*, 27214, https://doi.org/10.1038/s41598-024-77771-2.
17. Gutman, I.; Trinajstić, N. Graph theory and molecular orbitals. Total φ-electron energy of alternant hydrocarbons. *Chem. Phys. Lett.* **1972**, *17*, 535-538, https://doi.org/10.1016/0009-2614(72)85099-1.
18. Gutman, I.; Furtula, B.; Vukićević, Ž.K.; Popivoda, G. On Zagreb Indices and Coindices. *MATCH Commun. Math. Comput. Chem.* **2015**, *74*, 5-16.
19. Azari, M.; Iranmanesh, A. Computing the eccentric-distance sum for graph operations. *Discret. Appl. Math.* **2013**, *161*, 2827-2840, https://doi.org/10.1016/j.dam.2013.06.003.
20. Geng, X.; Li, S.; Zhang, M. Extremal values on the eccentric distance sum of trees. *Discret. Appl. Math.* **2013**, *161*, 2427-2439, https://doi.org/10.1016/j.dam.2013.05.023.
21. Hemmasi, M.; Iranmanesh, A.; Tehranian, A. Computing Eccentric Distance Sum for an Infinite Family of Fullerenes. *MATCH Commun. Math. Comput. Chem.* **2014**, *71*, 417–424.
22. Li, S.; Wu, Y. On the extreme eccentric distance sum of graphs with some given parameters. *Discret. Appl. Math.* **2016**, *206*, 90–99, https://doi.org/10.1016/j.dam.2016.01.027.
23. Li, S.C.; Wu, Y.Y.; Sun, L.L. On the minimum eccentric distance sum of bipartite graphs with some given parameters. *J. Math. Anal. Appl.* **2015**, *430*, 1149-1162, https://doi.org/10.1016/j.jmaa.2015.05.032.
24. Padmapriya, P.; Mathad, V. The eccentric-distance sum of some graphs. *Electron. J. Graph Theory Appl.* **2017**, *5*, 51-62, https://doi.org/10.5614/ejgta.2017.5.1.6.
25. Yu, G.; Feng, L.; Ilić, A. On the eccentric distance sum of trees and unicyclic graphs. *J. Math. Anal. Appl.* **2011**, *375*, 99–107, https://doi.org/10.1016/j.jmaa.2010.08.054.
26. Asghar, A.; Rafaqat, M. Investigating the Neighborhood Degree Based Topological Indices of Certain Isomeric Natural Polymers. *ACS Omega* **2025**, *10*, 3563-3574, https://doi.org/10.1021/acsomega.4c08243.
27. Jing, L.; Yousaf, S.; Farhad, S.; Tchier, F.; Aslam, A. Analyzing the expected values of neighborhood degree-based topological indices in random cyclooctane chains. *Front. Chem.* **2024**, *12*, 1388097, https://doi.org/10.3389/fchem.2024.1388097.
28. Zaman, S.; Ullah, A.; Naseer, R.; Rasool, K.B. Mathematical Concepts and Empirical Study of Neighborhood Irregular Topological Indices of Nanostructures $TUC_4C_8[p, q]$ and GTUC $[p, q]$. *J. Math.* **2024**, *2024*, 7521699, https://doi.org/10.1155/2024/7521699.
29. Thomas, S.; Somasekharan, L. Polyhedral Oligomeric Silsesquioxane (POSS) Polymer Nanocomposites: From Synthesis to Applications; Elsevier: **2021**; https://doi.org/10.1016/C2019-0-02011-0.
30. Xie, M.; Li, G.; Fan, W.; Li, M.; Sun, Q.; Guo, J.; Xia, S.; Fu, W. Low dielectric silsesquioxane-modified benzocyclobutene composites. *Polymer* **2023**, *282*, 126188, https://doi.org/10.1016/j.polymer.2023.126188.
31. Dielectric Constants. https://docs.materialsproject.org/methodology/materials-methodology/dielectricity (accessed on 6 January **2026**).
32. Leu, C.-M.; Chang, Y.-T.; Wei, K.-H. Synthesis and Dielectric Properties of Polyimide-Tethered Polyhedral Oligomeric Silsesquioxane (POSS) Nanocomposites via POSS-diamine. *Macromolecules* **2003**, *36*, 9122-9127, https://doi.org/10.1021/ma034743r.
33. Zhao, H.; Zhao, S.-Q.; Hu, G.-H.; Zhang, Q.-C.; Liu, Y.; Huang, C.-X.; Li, W.; Jiang, T.; Wang, S.-F. Synthesis and characterization of waterborne polyurethane/polyhedral oligomeric silsesquioxane composites with low dielectric constants. *Polym. Adv. Technol.* **2019**, *30*, 2313-2320, https://doi.org/10.1002/pat.4659.
34. Eckstorff, F.; Zhu, Y.; Maurer, R.; Müller, T.E.; Scholz, S.; Lercher, J.A. Materials with tunable low-k dielectric constant derived from functionalized octahedral silsesquioxanes and spherosilicates. *Polymer* **2011**, *52*, 2492-2498, https://doi.org/10.1016/j.polymer.2011.01.050.

## Publisher's Note & Disclaimer